

A TWO-STEP PARALLEL PLATE CHAMBER WITH A RESISTIVE GERMANIUM ANODE AND A TWO DIMENSIONAL READOUT FOR THE DETECTION OF MINIMUM IONIZING PARTICLES

R. BELLAZZINI, C. BETTI, A. BREZ, E. CARBONI, M.M. MASSAI and M.R. TORQUATI

Dipartimento di Fisica dell' Università di Pisa and

Istituto Nazionale di Fisica Nucleare, Sezione di Pisa Via Livornese 582/A – San Piero a Grado I – 56010 – Pisa – Italy

A parallel plate avalanche chamber specially suited for the high resolution detection of minimum ionizing particles (m.i.p.) is presented. The anode is made of a thin germanium layer with a sheet resistivity $>1 \text{ M}\Omega/\square$ while the cathode is made of a nickel mesh having 600 line pairs/in. A chess board of pads placed behind the anode plane is used to obtain the positional information. A 100% detection efficiency, a 40 ns (fwhm) time resolution and a spatial resolution better than $140 \mu\text{m}$ (fwhm) for both coordinates have been measured.

1. Introduction

Recently, parallel plate counters have received the renewed attention of several authors [1–4] as a possible alternative to wire chambers for the detection of minimum ionizing particles. Their major advantages when utilized as detectors of heavily ionizing particles are: (1) high spatial resolution in both the coordinates on the detection plane, (2) high data-rate capability, (3) good two track resolution, (4) insensitivity to radiation damage, (5) no thin fragile wires in the detector. Their major drawback was the low gas gain obtainable before sparking occurred and therefore a low spatial resolution and detection efficiency for minimum ionizing particles. To overcome these problems we have designed, built and tested a new type of parallel plate avalanche chamber. This detector has a resistive germanium anode and a high resolution two-dimensional read-out and works at atmospheric or higher pressure. To increase the detection efficiency a ionization and drift region several millimeters thick was added in front of a very thin amplification gap. Ionization electrons delivered by a traversing particle are drifted into the amplification gap where they are multiplied with a gain $\approx 10^5$. A nickel mesh having 600 line pairs per inch divides the two field regions. Because of its high resistivity, the anode is transparent to the fast impulse generated by the avalanche electrons. Behind the anode plane a chess-board like pattern of pads collects this fast pulse and it is used to obtain the positional sensitivity.

In this paper the principle of operation and preliminary results of laboratory tests of this detector with soft X-rays and cosmic rays are presented.

2. Principle of operation of the detector

A parallel plate chamber (PPC) consists of two planar electrodes mounted parallel to each other (see fig. 1). When a potential difference is applied to the narrow gap, a uniform, intense, electric field is established inside the detection volume. Ionization electrons delivered by a traversing particle start to multiply until they are collected by the anode. In the case of a point ionization the number of the secondary electrons is given by

$$n = n_0 e^{ad},$$

with n_0 = number of primary electrons d = drift length
 a = first Townsend coefficient.

The detection efficiency depends, therefore, on the number of primary electrons and on the gas gain e^{ad} . The ionization collision in a gas is a Poisson-like process. Assuming the detection of a single ionization cluster, six clusters are necessary to have 99.8% detection efficiency. In a argon (90%)–methane (10%) mixture at STP the mean ionization density is 2 clusters/mm. As the amplification gap is very thin (typically 2 mm) we have added a thick drift region with a moderate electric field in front of the amplification gap. Inside the drift gap a large number of primary electrons is created. These electrons drift into and are multiplied in the amplification region. A gas gain up to 10^4 – 10^5 can be obtained. The signal has an amplitude of a few hundreds of microvolts and consists of two parts:

- (1) a fast rising component due to the collection of the electrons,
- (2) a slow rising component due the positive ions with

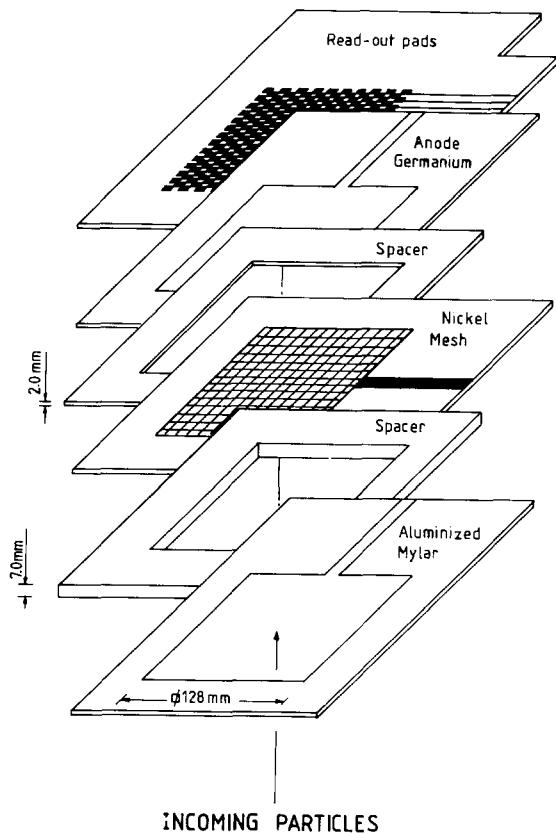


Fig. 1. Exploded view of the detector assembly.

their much lower drift velocity.

If the electrode plates of the amplification gap are both made of conducting material a voltage pulse due to the collection of the drifting charges can be observed in an external circuit connected to one of the electrodes. However, because the whole electrode plane moves to the new potential no information can be obtained from this signal.

The situation is completely different if one or both electrodes are made out of a semiconducting material with a sufficiently high sheet resistivity. In this case we can consider the electrodes as a two dimensional array of resistors. If an array (one or two dimensional) of capacitors is placed behind the resistive plane a "short circuit" to ground is established for fast rising currents. We can say that the resistive plane acts as conductor for dc currents, so that it can be charged to a suitable potential, while it acts as a dielectric for very short currents so that it is transparent to the corresponding pulses. The positional information can be obtained from the distribution of the charge collected on the external capacitors.

3. Detector design and construction

The material we choose for the construction of the resistive electrode is germanium. Germanium has a bulk resistivity of $60 \Omega \text{ cm}$. A $1\text{--}0.1 \mu\text{m}$ thick deposit obtained via vacuum evaporation, results in a sheet resistivity in the range $0.5\text{--}50 \text{ M}\Omega/\text{square}$ which is high enough to ensure full transparency for the fast component of the signal coming from the detector. Further advantages of the vacuum evaporation are the high uniformity in thickness of the deposit ($\pm 1\%$) and the easily controllable value of the resistivity which is only a function of the thickness of the deposit. The high uniformity of the sheet resistivity allows us to work at values of resistivity close to the one corresponding to the full transparency threshold, thus reducing the rate limitations of the device. As a support for the germanium deposit we used a machined epoxy plane or polished glass. The cathode is made of a $25 \mu\text{m}$ thick nickel mesh (manufactured by Buckbee-Mears Operation - USA) having wires $20 \mu\text{m}$ apart and a wire pitch of $35 \mu\text{m}$ (see fig. 2). The optical transparency of the mesh is 50%. A mesh with such a fine pitch was selected to have a uniform electric field over the entire gap. The gap between the anode and the cathode was obtained with spacers made out of epoxy having a thickness in the range of 1–3 mm. Special care was taken during the machining of the epoxy planes to ensure good planarity of the anode plate and a good uniformity of the spacer thickness ($\pm 0.005 \text{ mm}$ tolerance). The nickel foil was carefully stretched in order to avoid any wrinkles. The drift gap was achieved with a 7 mm thick spacer and a $5 \mu\text{m}$ thick aluminized mylar foil. This light material was chosen to have an entrance window transparent to short range particles such as low energy X- or β -rays. Behind the anode plane a double-sided board of 2×2 "pads" collects the fast electron pulses and is used to measure the position of the event. Half of the pads are connected in a zig-zag manner to form rows on one side

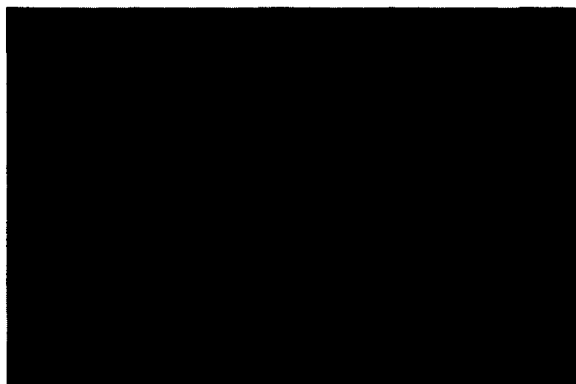


Fig. 2. Magnified detail of the nickel mesh having 600 line pairs/inch.

of the chess-board like pattern. Metallized holes of 0.5 mm diameter connect the remaining half of the pads to form columns on the back-plane of the chess-board. In this way a two-dimensional read-out is obtained looking at the detector from one side only, leaving the frontside free as a window for the incoming particles. The advantages of this set up are:

- (1) two dimensional positional information is obtained from an almost perfectly homogeneous, self triggering detector;
- (2) the detector and the read-out system are physically and logically separated so that they can be optimized independently;
- (3) the data rate is distributed over the entire detector volume;
- (4) the detector is mechanically very simple and sturdy (no fragile wires etc).

4. Results

The results described in this paper refer mainly to the operation of the chamber at standard pressure. For the detection efficiency measurement the chamber has also been operated for some time with up to 1.7 atm absolute pressure without any particular problem. The detector active area is $13 \text{ cm} \times 13 \text{ cm}$ and the gas filling was argon (90%)–methane (10%). A typical operating voltage when working at normal pressure was 3.2 kV corresponding to a uniform electric field of 16 kV/cm for a 2 mm gap. The drift field was normally set at 1 kV/cm. Under these conditions, according to Bunemann et al. [5], the mesh transparency for electrons should be 100%.

To study the detection efficiency for minimum ioniz-

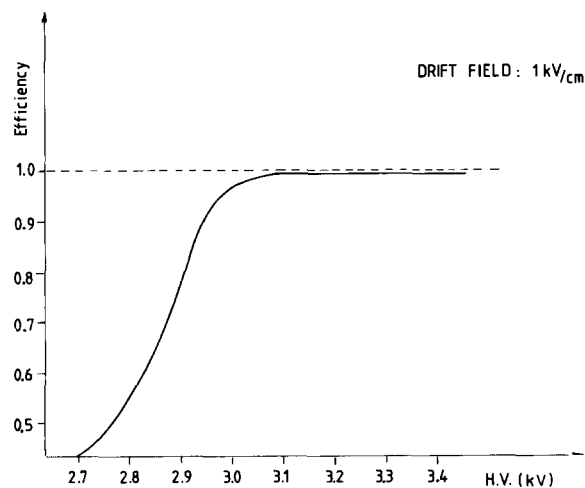


Fig. 3. The detection efficiency as a function of the applied voltage.

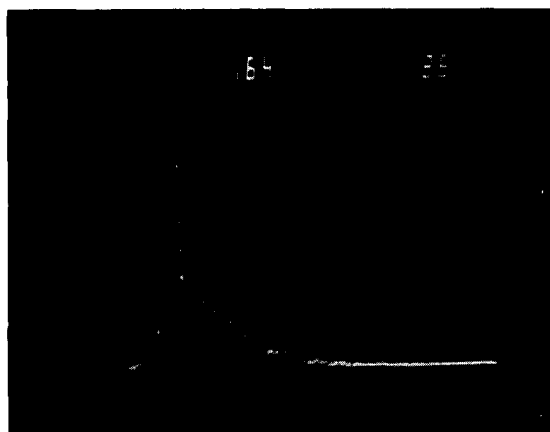


Fig. 4. Time resolution of the full detector (amplification and drift gap). Sensitivity: 320 ps/channel.

ing particles we have built a cosmic ray telescope made of two small plastic scintillators, A and B, placed above and below the PPC. Fig. 3 shows the coincidence ratio $A \cdot B \cdot \text{PPC} / A \cdot B$ as a function of the operating voltage. The full efficiency is reached starting from 3.0 kV. Onwards, a long plateau is observed. To study the intrinsic efficiency of the amplification gap we have reversed the polarity of the voltage on the entrance window to positive polarity and we have measured the ratio $A \cdot B \cdot \text{PPC} / A \cdot B$. At standard pressure the intrinsic detection efficiency at 3.2 kV was 20% for a 2 mm gap. At 1.5 atm absolute pressure the efficiency for a 2 mm gap increased to 75% at 4.47 kV.

The time resolution was measured using $A \cdot B$ as a start and $A \cdot B \cdot \text{PPC}$ as a stop signal to the time to amplitude converter. Fig. 4 shows the resulting pulse height spectrum. The fwhm is $\sim 40 \text{ ns}$. In order to

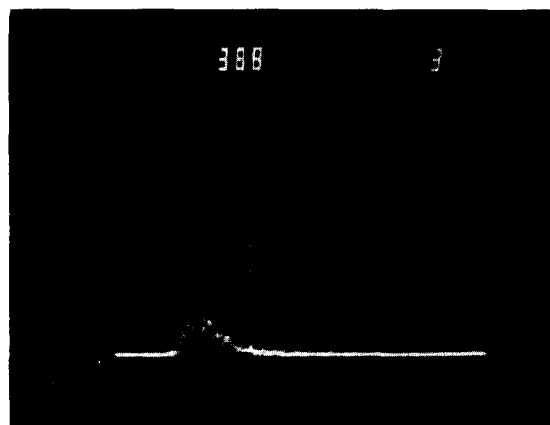


Fig. 5. Time resolution of the detector without the drift gap. Sensitivity: 160 ps/channel. The distance between the two vertical lines is 228 channels.

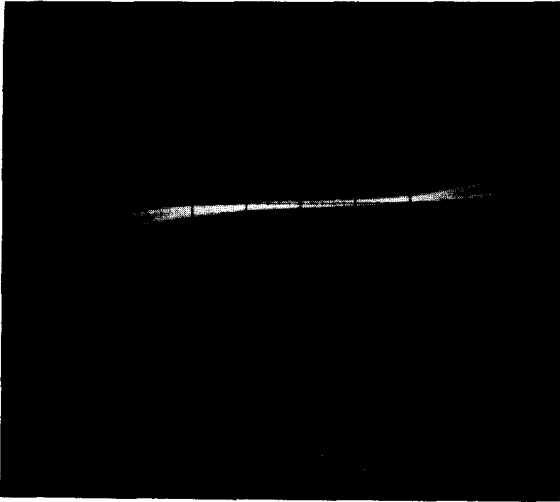


Fig. 6. The mesh signal when the chamber is irradiated with a ^{55}Fe source.

trigger the PPC discriminator a sufficient number of clusters has to be created. This gives rise to a time jitter as the coordinate of the point fluctuates. If only ionization clusters directly delivered into the amplification gap are accepted, the time resolution is much better as indicated by fig. 5. This is due to a reduction of the sensitive thickness to less than 1 mm.



Fig. 7. Pulse height spectrum of the signal of fig. 6.

The configuration of the PPC is conceptually similar to that of a proportional counter: an ionization and drift region followed by a much narrower amplification region. As such the PPC exhibits a good energy resolution. Fig. 6 shows the signal obtained from the nickel mesh when the chamber is irradiated with an ^{55}Fe source. The full energy peak (6 keV) and the escape peak (3 keV) are apparent. Fig. 7 shows the pulse height spectrum of the signal in fig. 6. The energy resolution was estimated to be 25% at 6 keV.

The event position is obtained from the measurement of the centroid of the charge distribution on the read-out pads. The electronic chain consists of a low noise charge preamplifier [6], a linear amplifier with a 2 μs gaussian shaping and a peak sensing ADC for each row and column. The data acquisition is started and gated by the prompt signal obtained from the mesh. The distance of the read-out plane from the anode plane can be easily adjusted depending on the pitch of the rows and columns. The relative gains of each chan-

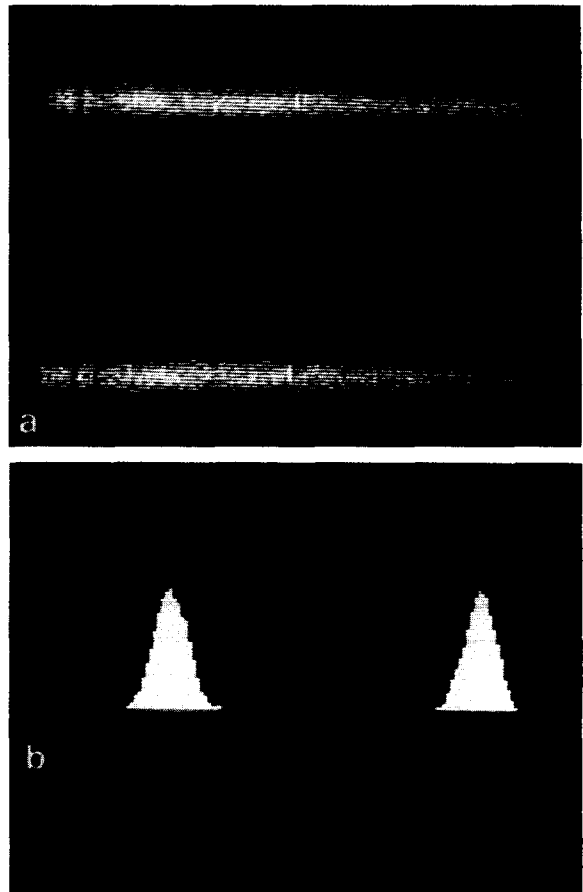


Fig. 8. (a) The reconstructed image of two slits 100 μm wide, 1.1 mm apart. (b) Histogram of a profile across the two slits. The width (fwhm) of the two peaks is $\approx 140 \mu\text{m}$.

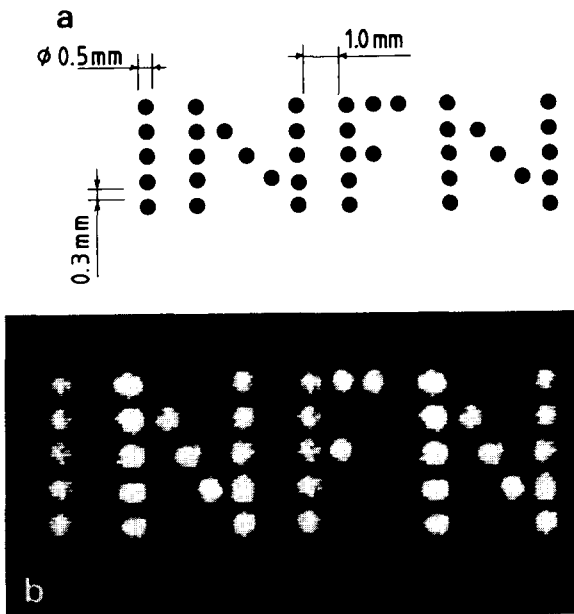


Fig. 9. (a) Resolution phantom consisting of 39 holes arranged to form the word INFN. (b) The reconstructed image.

nel were equalized within 1%. To measure the spatial resolution we built a resolution phantom consisting of two slits $100\ \mu\text{m}$ wide, 8 mm thick and 1.1 mm apart. It was uniformly illuminated with an ^{55}Fe source. Fig. 8 shows the reconstructed image together with the histogram of a profile across the two slits. The width (fwhm) of the two peaks is $\sim 140\ \mu\text{m}$. This figure includes the slit width, the range of the photo-electrons and the parallax error.

To study the two dimensional imaging capability we utilized a resolution phantom which is shown in fig. 9 together with the reconstructed image.

5. Discussion

We have presented a position sensitive parallel plate counter specially suited for the high resolution detection of minimum ionizing particles. By adding a wide gap drift region in front of a thin amplification gap a detection efficiency of 100% and a time resolution of 40 ns (fwhm) has been observed. The spatial resolution is $\approx 60\ \mu\text{m}$ (rms) for both the coordinates on the detection plane. The operation of the detector without the drift region improves the time resolution significantly (15 ns fwhm) but lowers the efficiency ($\approx 20\%$ for a 2 mm gap). The use of a gas with a higher ionization density and drift velocity like CF_4 or xenon should improve both the detection efficiency and the time resolution. On the other hand the operation of the detector at a pressure higher than atmospheric should improve not only the detection efficiency but also the spatial and time resolution. An increase of the detection efficiency from 20% to 75% when operating the detector at 1.5 atm absolute pressure has indeed been observed for a 2 mm gap.

We are studying several schemes to improve the rate capability of the detector which is limited by the voltage drop due to the discharge process. All these schemes rely on a distributed high voltage supply.

References

- [1] A. Peisert, Nucl. Instr. and Meth. 217 (1983) 229.
- [2] H.J. Hilke, Nucl. Instr. and Meth. 217 (1983) 189.
- [3] A. Peisert et al., IEEE Trans. Nucl. Sci. NS-31 (1984).
- [4] R. Bellazzini et al., IEEE Trans. Nucl. Sci. NS-33 (1986).
- [5] O. Bunemann et al., Can. J. Res. 27A (1949) 191.
- [6] V. Radeka, IEEE Trans. Nucl. Sci. NS-21 (1) (1974) 51.